# Computer-assisted proofs for chaotic and stability behaviour in dynamical systems

"Theses of PhD Dissertation"

Balázs Bánhelyi

Supervisor:
Dr. Tibor Csendes

University of Szeged
Szeged, 2007

# 1 Introduction

An important question is while studying approximations of the solutions of differential equations, whether the given problem has a stable solution or chaotic behaviour. We study verified computational methods to check regions the points of which fulfill the conditions of some given behaviour.

In this case the verification means mathematical strong verification. In the computational part, rounding and other errors were considered. Instead of real numbers, we can also calculate with intervals. In case the bounds of the result interval are not computer representable, then they are rounded outward.

Then, we show other technique—based on subset relations—which is able to prove the existence of a topological horseshoe and chaotic behaviour. The collection of the subset relations $\mathcal{T}_j(W_j) \subset U_j$ forms a sufficient condition for chaos in a region determined by the subset relations themselves (see Figure 1). In order to locate chaotic regions, one has to find the subset relations to be checked.

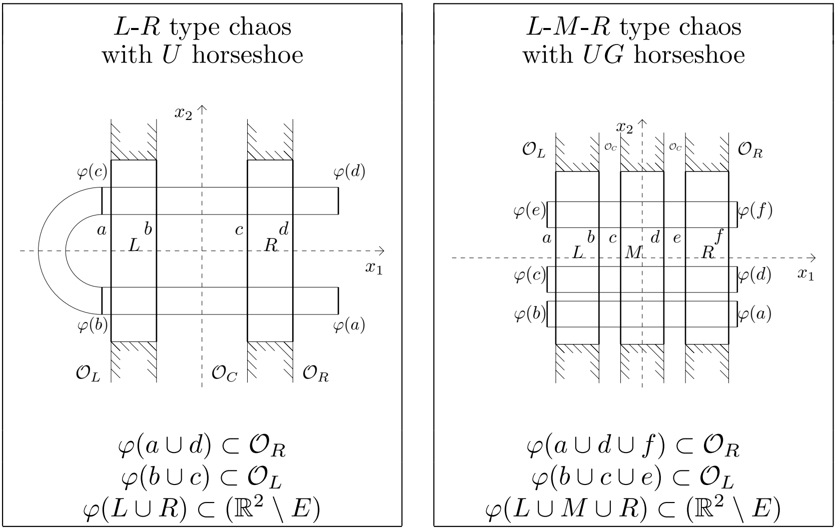


Figure 1: Some different Smale–horseshoes

## 2 Chaotic regions of the Hénon map

The problem is usually solved by careful studying the given problem with much human interaction, followed by an estimation of the Lipschitz constant, bounding the rounding errors to be committed, and finally a number of grid points are checked one by one by a proper computer program [15]. Instead of that, we introduce a new—interval arithmetic based—automatized method.

### 2.1 A checking algorithm

We study verified computational methods to check and locate regions the points of which fulfill the conditions of chaotic behaviour. The investigated Hénon mapping is

$$\mathcal{H}(x, y) = (1 + y - Ax^2, Bx).$$

Zgliczyński [15] considered the $A = 1.4$ and $B = 0.3$ values and some regions of the two dimensional Euclidean space: $E = E_1 \cup E_2 = \{(x, y) \mid x \geq 0.4,\ y \geq 0.28\} \cup \{(x, y) \mid x \leq 0.64,\ |y| \leq 0.01\}$, $\mathcal{O}_L = \{(x, y) \mid x < 0.4,\ y > 0.01\}$, $\mathcal{O}_R = \{(x, y) \mid y < 0\}$.

According to [15] Theorem 1 below ensures the chaotic behaviour for the points of the parallelograms $Q_0$ and $Q_1$ with parallel sides with the $x$ axis (for $y_0 = 0.01$ and $y_1 = 0.28$, respectively), with the common tangent of 2, and $x$ coordinates of the lower vertices are $x_a = 0.460$, $x_b = 0.556$; and $x_c = 0.558$, $x_d = 0.620$, respectively. The mapping and the problem details (such as the transformed sides of the parallelograms, $H^7(a)$, $H^7(b)$, $H^7(c)$, and $H^7(d)$) are illustrated on Figure 2.

**Theorem 1** (Zgliczyński)**.** *Assume that the following relations hold for the given particular Hénon mapping:*

$$\mathcal{H}^7(a \cup d) \subset \mathcal{O}_R, \tag{1}$$

$$\mathcal{H}^7(b \cup c) \subset \mathcal{O}_L, \tag{2}$$

$$\mathcal{H}^7(Q_0 \cup Q_1) \subset \mathbb{R}^2 \setminus E, \tag{3}$$

*then chaotic trajectories belong to the starting points of the regions $Q_0$ and $Q_1$ (see Figure 2).*

To check the inclusion relations required in Theorem 1 we have set up an adaptive subdivision algorithm based on interval arithmetic. First the

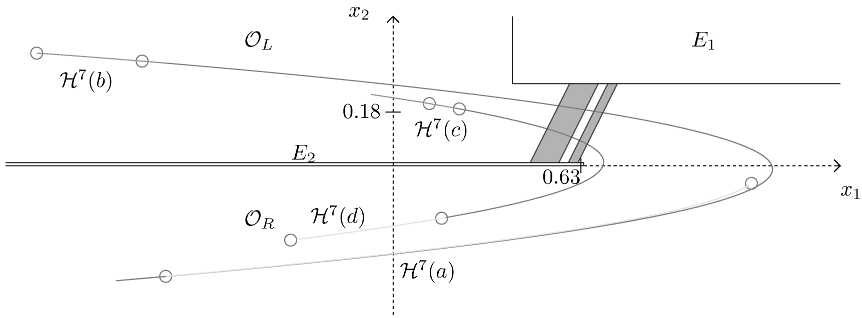


Figure 2: Illustration of the $H^7$ transformation for the classic Hénon parameters $A = 1.4$ and $B = 0.3$ together with the chaotic region of two parallelograms. The $a$, $b$, $c$, and $d$ sides of the parallelograms are depicted on the upper left picture of Figure 3.

algorithm determines the starting interval, that contains the region to be checked:

$$[0.46000000000, 0.75500000000] \times [0.01000000000, 0.28000000000].$$

Then the three conditions were checked one after the other. All of these proved to be valid—as expected. The number of function evaluations (for the transformation, i.e. for the seventh iterate of the Hénon mapping in each case) were 273, 523, and 1613, respectively. The algorithm stores those subintervals for which it was impossible to prove directly whether the given condition holds, these required further subdivision to achieve a conclusion (see Figure 3). The depth of the stack necessary for the checking was 11, 13, and 14, respectively. The CPU time used proved to be negligible, only a few seconds.

## 2.2 The accompanying optimization problem

We have proven that this algorithm is capable to provide the positive answer after a finite number of steps, and also that the given answer is rigorous in the mathematical sense. Once we have a reliable computer procedure to check the conditions of chaotic behavior of a mapping it is straightforward to set up an optimization model that transforms the original chaos location problem to a global optimization problem.

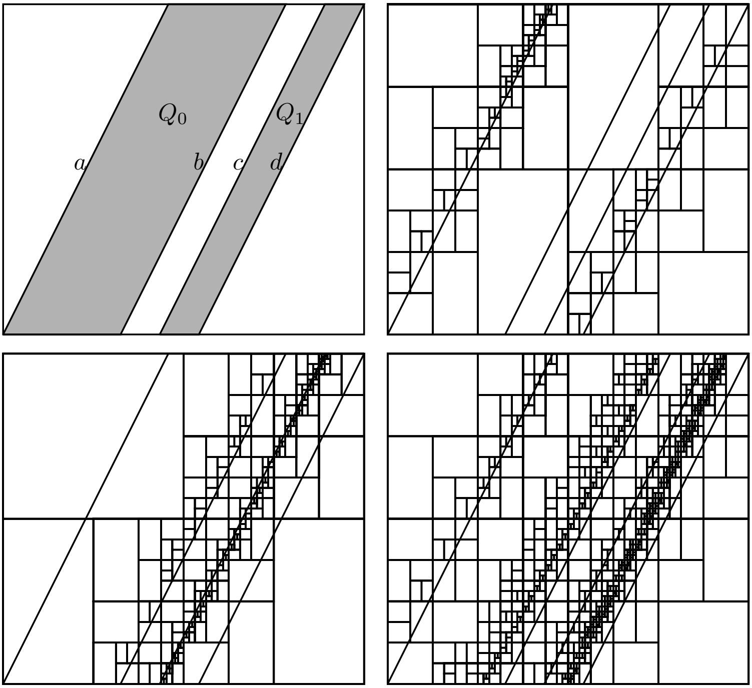


Figure 3: The parallelograms and the starting interval covered by the verified subintervals for which either the given condition holds (in the order of mentioning in Theorem 1), or they do not contain a point of the argument set.

The key question for the successful application of a global optimization algorithm was how to compose the penalty function. On the basis of earlier experiences collected with similar constrained problems, we have decided to add a nonnegative value proportional to how much the given condition was hurt, plus a fixed penalty term in case at least one of the constraints was not satisfied.

As an example, consider the case when one of the conditions for the transformed region was hurt, e.g. when (2), i.e. the relation

$$\mathcal{H}^k(b \cup c) \subset \mathcal{O}_1$$

does not hold for a given $k$th iterate, and for a region of two parallelograms. In such a case the checking routine will provide a subinterval that contains at least one point of the investigated region, and which contradicts the given condition. Then we have calculated the Hausdorff distance of the transformed subinterval $H^k(I)$ to the set $\mathcal{O}_1$ of the right side of the condition, $\max_{z \in H^k(I)} \inf_{y \in \mathcal{O}_1} d(z, y)$, where $d(z, y)$ is a given metric, a distance between a two dimensional interval and a point. Notice that the use of maximum in the expression is crucial, with minimization instead our optimization approach could provide (and has provided) result regions that do not fulfill the given conditions of chaotic behaviour. On the other hand, the minimal distance according to points of the aimed set (this time $\mathcal{O}_1$) is satisfactory, since it enables the technique to push the search into proper directions. In cases when the checking routine answered that the investigated subinterval has fulfilled the given condition, we have not changed the objective function.

Summing it up, we have considered the following bound constrained problem for the $T$ inclusion function of the mapping $\mathcal{T}$:

$$\min_{x \in X} g(x), \tag{4}$$

where

$$g(x) = f(x) + p\left(\sum_{i=1}^{m} \max_{z \in T(I)} \inf_{y \in S_i} d(z, y)\right),$$

$X$ is the $n$–dimensional interval of admissible values for the parameters $x$ to be optimized, $f(x)$ is the original, nonnegative objective function, and $p(y) = y + C$ if $y$ is positive, and $p(y) = 0$ otherwise. $C$ is a positive constant, larger than $f(x)$ for all the feasible $x$ points, $m$ is the number of conditions to be fulfilled, and $S_i$ is the aimed set for the $i$-th condition.

The emerging global optimization problem has been solved by the clustering optimization method.

| LO | ZO | FE | PE | T |
|---|---|---|---|---|
| 12 | 4 | 13,197 | 4,086 | 17 |
| 12 | 1 | 12,913 | 3,365 | 16 |
| 12 | 1 | 13,569 | 4,303 | 19 |
| 12 | 2 | 12,918 | 3,394 | 16 |
| 12 | 1 | 14,117 | 5,083 | 18 |
| 12 | 3 | 21,391 | 7,400 | 25 |
| 12 | 2 | 12,623 | 3,296 | 16 |
| 12 | 0 | 15,388 | 6,221 | 30 |
| 12 | 3 | 13,458 | 3,858 | 15 |
| 12 | 2 | 14,643 | 5,002 | 16 |

Table 1: Numerical results of the search runs (Here LO stands for the number of local optima found, ZO for the number of zero optimum values, FE for the number of function evaluations, PE for the number of penalty function evaluations, and finally T for the CPU time used in minutes.)

## 2.3 Applications

First, we have applied the global optimization model for the 5th iterate Hénon mapping. Note that the less the iteration number, the more difficult the related problem: no chaotic regions were reported for the iterates less than 7 till now. After some experimentation, the search domain set for the parameters to be optimized was:

$$A \in [1.00, 2.00],\ \ B \in [0.10, 1.00],$$

$$x_a, x_b, x_c, x_d \in [0.40, 0.64].$$

Table 1 presents the numerical results of the ten search runs.

We applied successfully this method to locate several chaotic regions of Hénon map (see Figure 4), and gave a lower bound for topological entropy. The topological entropy characterizes the mixing of points by the Hénon map. The numerical results are published in [2, 3, 4, 6, 5, 10, 12].

In this section my work is an implementation of the algorithm, the numerical results and integration of them.

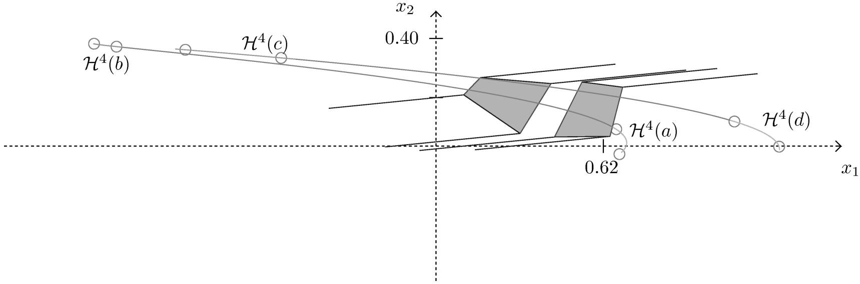


(a) 4th iterate of Hénon map.

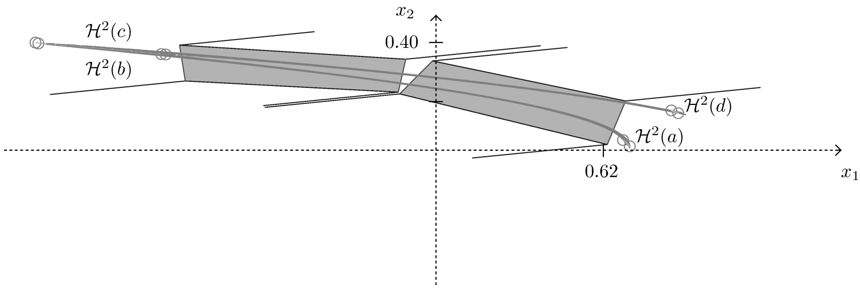


(b) 2nd iterate of Hénon map.

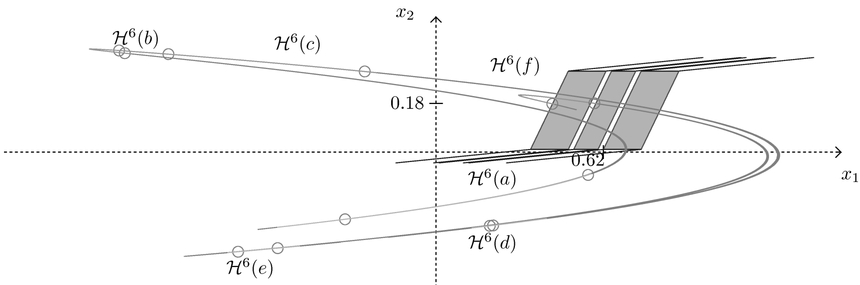


(c) 6th iterate of Hénon map.

Figure 4: Chaotic regions of Hénon map with classical parameters.

# 3 Chaotic behaviour of the forced damped pendulum

Recently, a few papers considered real dynamical problems and give a mathematical proof to chaotic behaviour. In this part we investigated a forced damped pendulum as the mechanical model and proof a Chaotic behaviour of them [13]. The curiosity thing in this problem that, we can give a one-to-one correspondence the chaotic behaviour and the gross behaviour of pendulum.

## 3.1 The forced damped pendulum

Consider a forced damped pendulum, i.e. we have a body on a weightless solid rod, forced to move on a vertical circle around the center point (see Figure 5). The mass and the length of the pendulum are equal to 1. We have a not negligible friction depending on the speed of the pendulum with a friction factor of $b = 0.1$. An external periodic force is applied to the body, $\cos t$, where $t$ is the time (it is independent of all other factors).

The related second order differential equation is

$$x'' = \cos t - 0.1x' - \sin x,$$

where $x$ is the angle of the pendulum, and $x'$ is the angle speed of the pendulum. The corresponding system of first order differential equations is

$$\begin{aligned} u' &= v, \\ v' &= \cos t - 0.1v - \sin u, \end{aligned}$$

where $u$ is the angle of the pendulum, and $v$ is the angle speed of the pendulum.

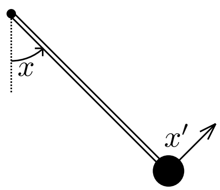


Figure 5: Illustration of Pendulum

We can formalize the chaotic behaviour in the following form:

**Theorem 2** (J.H. Hubbard). *Suppose we are given a biinfinite sequence $\epsilon_{k\in\mathbb{Z}} \in \{-1;0;1\}^Z$ arbitrarily chosen. Then the forced damped pendulum described by equation has at least one motion that corresponds to the biinfinite sequence $\epsilon_{k\in\mathbb{Z}}$ in the sense that during the time interval $[2k\pi, 2(k+1)\pi]$ the pendulum*

- *crosses the bottom position exactly once clockwise if and only if $\epsilon_k = -1$,*
- *does not crosses the bottom position at all if and only if $\epsilon_k = 0$,*
- *crosses the bottom position exactly once counterclockwise if and only if $\epsilon_k = 1$,*

*and does not point downwards at the time instant $t = 2k\pi$, $k \in Z$.*

## 3.2 Proof of chaos in a forced damped pendulum

First, We report on the first steps made towards the computational proof of the chaotic behavior of the forced damped pendulum. Although chaos was long conjectured for this differential equation, and it has been considered as plausible based on numerical simulation results, the rigorous proof is still missing.

In the proof we will need certain quadrilaterals $\{Q_k\}_{k\in\mathbb{Z}}$ "long" in the unstable and "short" in the stable directions so that there are *"exceptional" orbits* of the Poincaré mapping $P$ with the following properties:

- an exceptional orbit is contained in $\cup_{k\in\mathbb{Z}} Q_k$;
- an exceptional orbit visits the quadrilaterals consecutively: if $P^n(x_0, x_0') \in Q_k$ for some $k, n \in \mathbb{Z}$, then either $P^{n+1}(x_0, x_0') \in Q_{k-1}$ or $P^{n+1}(x_0, x_0') \in Q_k$ or $P^{n+1}(x_0, x_0') \in Q_{k+1}$.

In the main step of the proof of chaotic behaviour we will show that for an arbitrary consecutive order $\{Q_{i_k}\}_{k\in\mathbb{Z}}$ of quadrilaterals there is an exceptional orbit visiting the quadrilaterals in the prescribed order. To this end we have to know forward images $P(Q_k)$ (see Figure 6) and prove the existence of topological horseshoe.

We applied the earlier mentioned subdivision method, which is able to prove the chaotic behaviour of the considered systems. The details of the proof was published in [7, 8, 11]. In this section my work is a development and implementation of the computer assisted proof.

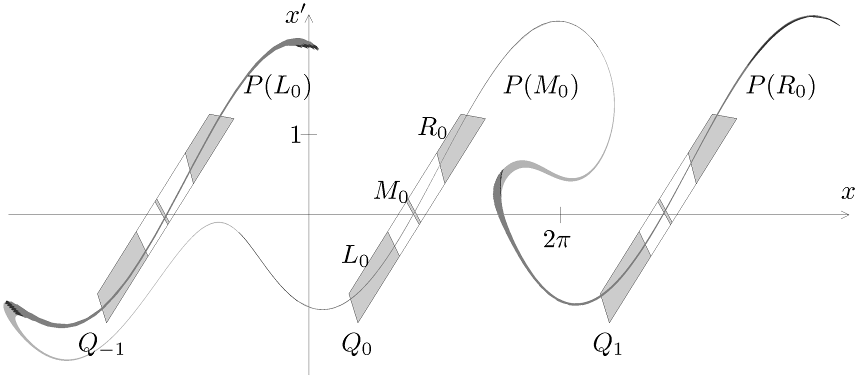


Figure 6: Forward Poincaré map in $t = \pm 2\pi$ time points of $Q_0$.

# 4 Investigation of Wright conjecture

E.M. Wright conjectured in a paper [14] published in 1955 that all solutions of a delay differential equation converge to zero for a wide set of the parameter $\alpha$. He gave a proof of the statement for $\alpha$ values between 0 and 1.5 and conjectured to be true for further $\alpha$ values below $\pi/2$.

## 4.1 Technique to following trajectory

E.M. Wright considered the delay differential equation

$$z'(t) = -\alpha z(t-1)(1 + z(t)),$$

where $\alpha$ is a positive number, and the initial function $\phi(s)$ is a constant, $c > -1$, i.e. $\phi(s) = c$ for $s \in [-1, 0]$.

To simplify the further calculations use the substitution $z(t) = e^{y(t)} - 1$. Then $z'(t) = e^{y(t)} y'(t)$ and $z(t-1) = e^{y(t-1)} - 1$. We obtain the delay differential equation

$$y'(t) = -\alpha \left( e^{y(t-1)} - 1 \right),$$

where the initial function is $\phi(s) = c$, $s \in [-1, 0]$.

When $\alpha \leq 1.5$, it is known, that the trajectory converges to zero, and when $\alpha \geq \pi/2$, the trajectory converges to different periodic solutions too (see Figure 7). In the following only the $\alpha \in [1.5, \pi/2]$ cases are

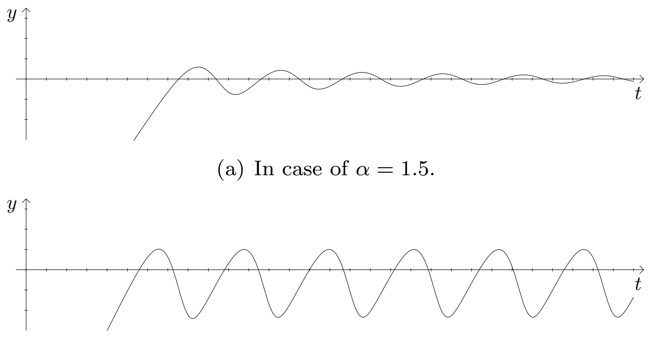

(a) In case of $\alpha = 1.5$.

(b) In case of $\alpha = 2.0$.

Figure 7: Illustration of trajectories.

investigated. On the basis of the collected numerical experience, we can expect that these solutions behave just like in the $\alpha \leq 1.5$ cases.

The analysis of the convergence to zero is very hard with numerical methods, so we consider an easier problem. We are interested in checking whether for all $\alpha \in \left[\frac{3}{2}, \frac{\pi}{2}\right]$, there exists a unit length time segment where the absolute value of the solution is less than 0.075.

Most verified techniques for solving ordinary differential equations apply a Taylor series. Our technique is based on the same idea too. The Taylor–series is:

$$y(x) = \sum_{k=0}^{n-1} \frac{(x - x_0)^k y^{(k)}(x_0)}{k!} + r_n.$$

Using the mean–value theorem, $r_n$ can be bounded by

$$r_n = \frac{(x - x_0)^n}{n!} y^{(n)}(x^*),$$

for some $x^* \in [x_0, x]$ $(x_0 \leq x)$.

If we want a better approximation of the solution, we have to use higher derivatives. We can characterize the higher derivatives with this formula:

$$y^{(k)}(t) = -\alpha y^{(k-1)}(t-1) + \sum_{i=1}^{k-1} \left( \begin{array}{c} k-2 \\ i-1 \end{array} \right) y^{(i)}(t-1) y^{(k-i)}(t).$$

To provide a mathematical proof, it is not enough to use Interval Arithmetic, we have to use the formula in a correct form. We can use the Taylor–series to bound the results:

$$Y(t_1) = \sum_{i=0}^{n-1} Y^i(t_0)\frac{(t_1-t_0)^i}{i!} + Y([t_0,t_1])^n\frac{(t_1-t_0)^n}{n!},$$

$$Y([t_0,t_1]) = \sum_{i=0}^{n-1} Y^i(t_0)\frac{([0,t_1-t_0])^i}{i!} + Y([t_0,t_1])^n\frac{([0,t_1-t_0])^n}{n!}.$$

In the algorithm, we use two fix length lists to store the solution bounds. The first list contains the solution and the derivatives on time intervals, which cover the unit length time segment. The other list stores the solution and the derivatives in concrete time points. We calculate the new elements of the lists with earlier discussed formula. The oldest elements are deleted from the lists, and the new ones are inserted. This technique has three parameters: step length, maximum derivate rank, and a precision of the interval arithmetic.

We proved the above statement for some tiny intervals around certain computer representable numbers, but we were not able to prove it for all points of the $\alpha$ parameter interval. This method published in [1].

## 4.2 Proof for a conjecture

In this section we describe and prove the correctness of a new, even more stronger bounding scheme that allows an efficient shrinking of the possible extreme values of a periodic solution.

The present approach follows another line of thought, still it is a kind of direct extension of that of Wright. Denote three subsequent zeroes of the trajectory by $t_0$, $t_0'$, and $t_0''$. Let us define functions bounding the trajectories. The trajectory bounding functions are illustrated by dashed lines on Figure 8.

The trajectory bounding functions will be sharpened sequentially, in an iterative way, i.e. the bounding functions of the time interval $(inc, 1)$ will be used to improve the bounding function on the interval $(dec, n)$, etc. Then, the bounding function of the last interval, $(inc, n)$ will be used to make the inequalities for the interval $(inc, 1)$ sharper, and so on. Those bounding function improvements that are based on a single bounding function of the earlier time interval are basically similar to the original technique used by Wright. The sharpening steps using two bounding functions on the

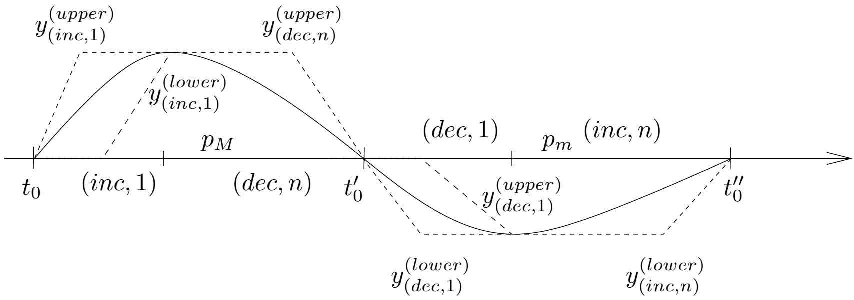


Figure 8: The trajectory bounding functions shown as dashed lines.

argument interval apply a new, Taylor series based method. At start we set the upper bounding functions to constant $M$, the lower bounding functions to $(-m)$ with the exceptions of $y^{(lower)}_{(inc,1)} = 0$ and $y^{(upper)}_{(dec,1)} = 0$. For all the six bounding functions we subdivide the unit length intervals to equal subintervals. On such a subinterval the bounding function is represented by a conservative constant value.

The conditions we check at the end of each iteration cycle of the bounding function sharpening procedure are

$$y^{(upper)}_{(inc,1)}(t_0 + 1) < M \quad \text{and} \quad -m < y^{(lower)}_{(dec,1)}(t'_0 + 1).$$

In case at least one of these conditions are fulfilled then the solution of the investigated delay differential equation cannot have a periodic solution with a maximal value of $M$ and the minimal value of $(-m)$ as assumed for the given $\alpha$ parameter.

After the theoretical investigations the remaining problem to be solved is to prove that for $\alpha$ values between 1.5 and $\pi/2$ no periodic solution exists with $M$ and $m$ absolute extreme values larger than a certain positive number. We illustration the connection between this two part on Figure 9. We applied a multithread B&B procedure, which is able to prove the remaining problem so—together with the theoretical part—we prove Wright original conjecture. The computer part of the proof is published in [9]. In this section my work is the estimation scheme—based on Wright's proof—and implementation of them.

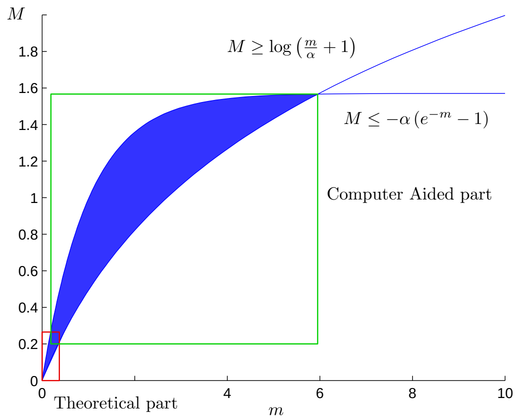


Figure 9: Illustration of the Theoretical part and Computer Aided part in proof.

# References


[1] B. Bánhelyi. The investigation of a delay differential equation by a verified computer procedure (in Hungarian: Egy késleltetett differenciálegyenlet vizsgálata megbízható számítógépes eljárással). *Alkalmazott Matematikai Lapok*, 24:131–150, 2007.

[2] B. Bánhelyi and T. Csendes. A verified computational technique to locate chaotic regions of Hénon systems. In *Proceedings of the 6th International Conference on Applied Informatics (ICAI2004), Eger*, pages 297–304, 2004.

[3] B. Bánhelyi and T. Csendes. A global optimization model for locating chaos: numerical results. In *Proceedings of the International Workshop on Global Optimization (GO05), Almería (Spain)*, pages 35–39, 2005.

[4] B. Bánhelyi, T. Csendes, and B.M. Garay. Optimization and the Miranda approach in detecting horseshoe-type chaos by computer. *International Journal of Bifurcation and Chaos*, 2007. Accepted for publication.

[5] B. Bánhelyi, T. Csendes, and B.M. Garay. $\Sigma_2$ chaos for iterates of the classical Hénon mapping. Manuscript, 2007.

[6] B. Bánhelyi, T. Csendes, and B.M. Garay. A verified optimization technique to bound topological entropy rigorously. In *Proceedings of 12th GAMM - IMACS International Symposium on Scientific Computing, Computer Arithmetic and Validated Numerics (SCAN 2006), Duisburg (Germany)*. IEEE, 2007. Accepted for publication.

[7] B. Bánhelyi, T. Csendes, B.M. Garay, and L. Hatvani. A computer-assisted proof for $\Sigma_3$-chaos in the forced damped pendulum equation. Manuscript, 2007.

[8] B. Bánhelyi, T. Csendes, B.M. Garay, and L. Hatvani. Computer assisted proof of chaotic behaviour of the forced damped pendulum. In *Proceedings of Colloquium on Differential and Difference Equations (CDDE2006), Brno (Czech Republic)*, Folia Facultatis Scientiarium Naturalium Universitatis Masarykianae Brunensis. Mathematica. Masaryk University, 2007. Accepted for publication.

[9] B. Bánhelyi, T. Csendes, T. Krisztin, and A. Neumaier. Proof for a conjecture of Wright on a delay differential equation II. – Computer Aided Part. Manuscript, 2007.

[10] T. Csendes and B. Bánhelyi. A global optimization model for locating chaos. In *Proceedings of the International Workshop on Global Optimization (GO05), Almería (Spain)*, pages 81–85, 2005.

[11] T. Csendes, B. Bánhelyi, and L. Hatvani. Towards a computer-assisted proof for chaos in a forced damped pendulum equation. *Journal of Computational and Applied Mathematics*, 199:378–383, 2007.

[12] T. Csendes, B.M. Garay, and B. Bánhelyi. A verified optimization technique to locate chaotic regions of a Hénon system. *Journal of Global Optimization*, 35:145–160, 2006.

[13] J. Hubbard. The forced damped pendulum: Chaos, complication and control. *Amer. Math. Monthly*, 106:741–758, 1999.

[14] E.M. Wright. A non-linear difference-differential equation. *Journal für die Reine und Angewandte Mathematik*, 194:66–87, 1955.

[15] P. Zgliczyński. Computer assisted proof of the horseshoe dynamics in the Hénon map. *Random Comput. Dynam.*, 5:1–17, 1997.

---

The published papers are available on
*www.inf.u-szeged.hu/∼banhelyi/Disszertacio* web page.